

# Distributed Hierarchical Temporal Memory with Shared Associative Memory for Cross-Entity Preemptive Warning

Pavia Bera<sup>a,\*</sup>, Jennifer Adorno<sup>a</sup>, Sanjukta Bhanja<sup>a</sup>

<sup>a</sup>*University of South Florida, Tampa, FL, USA*

---

## Abstract

Anomaly detection in multivariate time series remains a critical challenge in large-scale distributed systems, where related entities may exhibit transferable precursor behavior prior to anomaly onset. Existing methods typically operate independently on each data stream and therefore remain fundamentally reactive. To address this limitation, we introduce Distributed Hierarchical Temporal Memory (D-HTM), a neuromorphic framework that enables cross-entity preemptive warning through a Shared Associative Memory (SAM).

D-HTM combines a Spatial Pooler (SP) that projects observations into a common Sparse Distributed Representation (SDR) space, Temporal Memory (TM) modules that learn entity-specific dynamics online, and a Shared Associative Memory that stores recurring pre-anomaly signatures. By reusing precursor knowledge across related entities, D-HTM can issue warnings prior to local anomaly onset while preserving HTM's online learning capabilities.

We evaluate D-HTM on the Server Machine Dataset (SMD), the Soil Moisture Active Passive (SMAP) dataset, the Mars Science Laboratory (MSL) dataset, and a synthetic cascade benchmark designed to isolate precursor transfer. Experimental results demonstrate effective cross-entity warning propagation while maintaining competitive reactive anomaly detection performance. Across the real-world datasets, D-HTM provides an average warning lead time of 8.1 samples prior to anomaly onset.

These findings demonstrate that transferable precursor structure can

---

\*Corresponding author.

*Email address:* paviabera@usf.edu (Pavia Bera)

emerge within a shared SDR space and be reused for preemptive warning generation, extending HTM beyond isolated reactive detection toward distributed predictive reasoning.

*Keywords:* Hierarchical Temporal Memory, Shared Associative Memory, Multivariate Time Series Anomaly Detection, Cross-Entity Warning Propagation, Neuromorphic Computing

---

## 1. Introduction

The explosive growth in data generation from internet-connected devices has placed unprecedented demands on intelligent systems to process information efficiently and in real time. While traditional neural networks and other artificial intelligence (AI) algorithms have achieved remarkable success in domains such as image recognition and natural language processing, they face significant limitations when adapting to continuous, dynamic streams of unlabeled data [1]. These systems typically rely on batch learning, requiring extensive training data, computational resources, and retraining when the input distribution changes. Moreover, their architectures are not inherently designed for online inference and adaptation, which are critical requirements in applications such as anomaly detection, robotics, and streaming data analysis.

In contrast, Hierarchical Temporal Memory (HTM) is a biologically inspired framework modeled on the structure and function of the human neocortex. HTM learns continuously from streaming data by forming sparse distributed representations and temporal associations without requiring offline retraining [2, 3]. Its online learning capability has enabled applications in anomaly detection, robotics, forecasting, medical imaging, wafer inspection, biometric recognition, and environmental monitoring [4, 5, 6, 7, 8, 9, 10, 11].

At the core of HTM is the Temporal Memory (TM), which models key processing mechanisms of pyramidal neurons within the neocortex [11, 12], as illustrated in Fig. 1. Through interactions among proximal, distal, and apical dendrites, TM learns predictive associations between successive sparse activation patterns, enabling continuous temporal learning and anomaly detection without offline retraining [2, 12, 13].

Despite these strengths, HTM deployments in large-scale distributed environments remain fundamentally isolated. Each HTM agent learns only from its own local observations, even though anomalies in real-world sys-

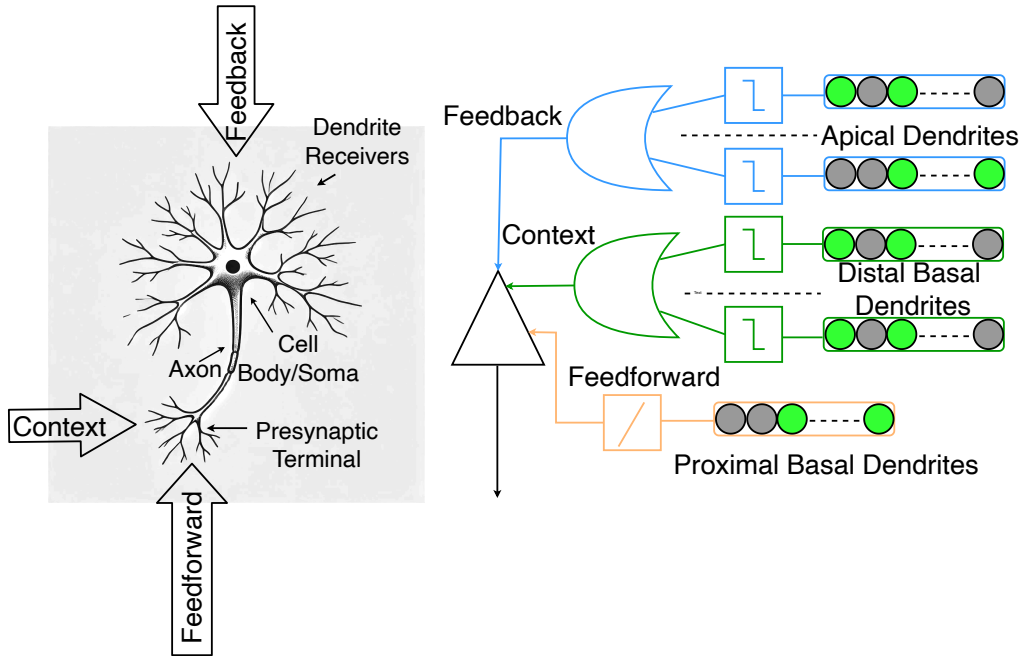


Figure 1: Comparison of biological and HTM neurons, highlighting feedback, feedforward, and contextual connections in both systems.

tems frequently propagate across related entities [14]. Consequently, existing anomaly detection methods, including state-of-the-art approaches such as OmniAnomaly [15], process each data stream independently and cannot exploit knowledge acquired elsewhere in the system. Anomaly detection therefore remains largely reactive, with each agent responding only after anomalous behavior becomes observable within its own data stream.

To address this limitation, we propose Distributed Hierarchical Temporal Memory (D-HTM), a framework that augments distributed HTM agents with a Shared Associative Memory (SAM). SAM stores recurring precursor activation patterns observed before anomaly onset and enables this knowledge to be shared across agents. When a local temporal pattern resembles a previously stored precursor, the retrieved memory contributes evidence toward a pre-emptive warning before local anomaly scores reach detection thresholds, allowing experience acquired by one entity to improve situational awareness across the network.

Unlike centralized monitoring architectures, D-HTM preserves HTM’s on-line learning capability by allowing each agent to learn independently while asynchronously querying and updating the shared associative memory. No

global synchronization or model retraining is required.

The main contributions of this paper are as follows:

- We introduce a Shared Associative Memory (SAM) that stores and retrieves recurring pre-anomaly sparse activation patterns, enabling transferable precursor knowledge across distributed HTM agents.
- We propose an inference-time cross-entity warning mechanism in which retrieved precursor memories generate pre-emptive warnings before local anomaly scores reach detection thresholds.
- We evaluate the proposed framework on the SMD, SMAP, and MSL benchmarks, demonstrating competitive reactive anomaly detection while showing that shared associative memory enables effective cross-entity warning propagation.

The remainder of this paper is organized as follows. Section 2 reviews related work on HTM, distributed anomaly detection, and neuromorphic computing. Section 3 introduces the HTM components relevant to this work. Section 4 presents the proposed Distributed HTM framework and the Shared Associative Memory. Section 5 reports the experimental evaluation, and Section 6 concludes the paper.

## 2. Related Work

Anomaly detection in distributed multivariate systems has been studied from several perspectives, including distributed learning, biologically inspired computing, and proactive anomaly detection. This section reviews the most relevant work and highlights the gap addressed by the proposed Shared Associative Memory (SAM) framework.

**Distributed and cooperative anomaly detection:** Multi-agent learning has been widely investigated as a means of improving scalability and robustness in complex monitoring environments [16, 17]. Classical distributed systems rely on centralized controllers or shared replay buffers, while more recent biologically inspired approaches emphasize decentralized coordination in which agents learn locally and periodically exchange information [18]. In temporal sequence modeling, distributed learning has primarily been built upon recurrent neural networks and attention-based architectures [19, 20], which require offline gradient-based optimization and are not inherently designed for continual online adaptation.

Federated learning (FL) has emerged as the dominant paradigm for distributed multivariate anomaly detection, allowing local models to be trained independently while exchanging only model updates [21]. Recent work has extended this idea through multi-task federated learning [22], hypernetwork-based aggregation [23], IIoT intrusion detection [24], and LLM-based multi-agent coordination [25, 26]. Complementing these, Audibert *et al.* [14] demonstrated that anomalies in complex distributed systems rarely occur in isolation, with failure signatures frequently propagating across related machines. Similarly, attempts to scale HTM to distributed environments have relied primarily on centralized coordination or static partitioning [27], without providing a mechanism for sharing learned temporal knowledge across agents.

Despite their differences, existing distributed approaches communicate primarily during *training* by exchanging gradients, model parameters, or task-level information. During online inference, each agent operates independently, with no mechanism to propagate learned precursor patterns to neighboring agents before local anomaly onset. This distinction fundamentally separates the proposed inference-time warning mechanism from existing distributed learning approaches.

**Biologically inspired and neuromorphic approaches:** Hierarchical Temporal Memory (HTM) is a biologically inspired framework that models neocortical computation using Sparse Distributed Representations (SDRs) and online temporal learning [27, 28]. Its ability to learn continuously without retraining has made HTM well suited for streaming analytics and anomaly detection [29]. Complementary neuromorphic approaches, including spiking neural networks and specialized hardware such as Loihi [30, 31, 32], likewise exploit sparse asynchronous computation for continual temporal inference. However, these biologically inspired systems remain predominantly single-agent and do not support sharing learned anomaly patterns across independently operating agents in real time.

**Proactive and pre-emptive anomaly detection:** A complementary line of research focuses on detecting anomalies before they fully manifest. Early work by Thottan and Ji [33] introduced distributed proactive monitoring using intelligent agents, while RePAD [34] extended this concept through online LSTM-based prediction for streaming time series. More recently, forecasting-based proactive methods [35], factor-graph reasoning for intrusion detection [36], and early-detection benchmarks [37] have demonstrated that meaningful precursor information can often be identified before

anomaly onset.

Nevertheless, these approaches remain fundamentally single-stream. Early warnings are generated solely from observations within the local data stream, and no mechanism exists for transferring learned precursor knowledge across related entities. This limitation also applies to federated methods, where communication is restricted to model updates and does not occur during online inference.

**Benchmarks and evaluation:** The Server Machine Dataset (SMD) [15], together with the SMAP and MSL telemetry benchmarks, has become the standard evaluation suite for multivariate time-series anomaly detection. OmniAnomaly, introduced alongside these datasets, remains one of the most widely used reactive baselines for anomaly detection [15]. Subsequent methods, including InterFusion [38] and StackVAE [39], have further improved reactive detection performance under the standard evaluation protocols. These methods, however, are designed for single-entity anomaly detection and therefore provide the reactive baselines against which the proposed cross-entity warning framework is evaluated.

Table 1 summarizes the key architectural differences between representative anomaly detection approaches and the proposed SAM framework. The comparison emphasizes the properties most relevant to this work, including online learning capability, per-machine deployment, cross-agent communication, and support for pre-emptive warning generation.

Table 1: Comparison of distributed and cooperative anomaly detection methods. **Bold** highlights the differentiating properties of the proposed SAM framework. ✓ = yes; × = no.

Method	Paradigm	Per-mach.	On-line	Cross-agent communication	Pre-empt.
OmniAnomaly [15]	Stochastic RNN (VAE+NF)	×	×	None	×
InterFusion [38]	Hierarchical VAE	×	×	None	×
StackVAE [39]	Stacked VAE + GNN	×	×	None	×
USAD [14]	Dual-AE adversarial	×	×	None	×
RePAD [34]	LSTM online prediction	×	✓	None	✓
Jeon et al. [35]	Forecasting proactive	×	×	None	✓
uFedHy [23]	Federated hypernetwork	✓	×	Gradient aggregation (train-time)	×
SADMC [22]	Multi-task federated FL	✓	×	Gradient aggregation (train-time)	×
MAS-LSTM [24]	Decentralized LSTM + GSP	✓	×	None (parallel agents)	×
AD-AGENT [25]	LLM pipeline orchestration	×	×	Workflow memory (train-time)	×
LEMAD [26]	Hierarchical LLM-MAS	✓	×	Task delegation (train-time)	×
<b>SAM (ours)</b>	<b>HTM + Shared Associative Memory</b>	✓	✓	<b>Associative precursor memories (inference-time)</b>	✓

As summarized in Table 1, existing distributed anomaly detection methods exchange gradients, model parameters, or task-level information during

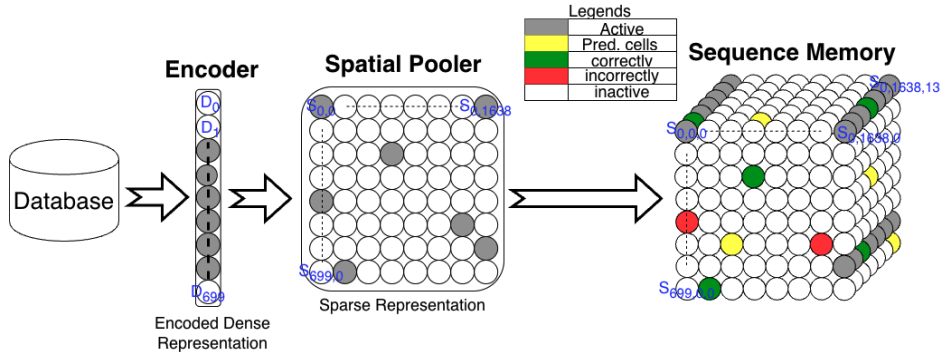


Figure 2: Overview of the Hierarchical Temporal Memory (HTM) architecture, including the encoder, Spatial Pooler (SP), and Temporal Memory (TM).

training, while proactive methods generate warnings only from the local data stream. In contrast, the proposed SAM framework introduces inference-time communication through retrieval of previously learned precursor memories. Rather than sharing model parameters, agents share transferable temporal knowledge encoded as sparse precursor patterns, enabling early warnings to propagate across related entities before local anomaly onset. “`latex id="a7mw0s"`

### 3. Background

Hierarchical Temporal Memory (HTM) is a biologically inspired machine learning framework modeled after the mammalian neocortex. Unlike conventional deep learning methods that require offline training and periodic retraining, HTM continuously learns from streaming data while simultaneously performing inference. As illustrated in Fig. 2, the HTM pipeline consists of three components: an encoder, a Spatial Pooler (SP), and a Temporal Memory (TM), which together transform raw observations into sparse representations and learn their temporal relationships.

The encoder converts raw numerical, categorical, or spatial inputs into Sparse Distributed Representations (SDRs), high-dimensional binary vectors containing only a small fraction of active bits. SDRs preserve semantic similarity through overlapping active bits while remaining robust to noise and small perturbations. More importantly for this work, their sparse overlap statistics make random matches exceedingly unlikely, providing a reliable basis for overlap-based similarity matching across entities.

The Spatial Pooler maps encoder-generated SDRs into a fixed population of sparse mini-columns using k-Winners-Take-All inhibition and local Hebbian-like learning. Similar inputs therefore activate overlapping column subsets, producing a stable sparse representation that preserves input similarity while reducing sensitivity to noise. In the proposed framework, this property enables different entities to share a common representation space suitable for cross-entity comparison.

Temporal Memory extends HTM into the temporal domain by learning transitions between successive Spatial Pooler activations. By forming predictive associations between sparse activation patterns, TM performs continuous sequence learning and produces anomaly scores from prediction errors without requiring offline retraining.

The proposed framework relies on three key properties of HTM: (i) SDRs provide robust sparse representations with reliable overlap statistics, (ii) the Spatial Pooler maps similar inputs to comparable sparse activations, and (iii) Temporal Memory continuously learns temporal structure while detecting anomaly onset through prediction errors. Together, these properties enable the storage, retrieval, and transfer of recurring precursor patterns across distributed entities, forming the foundation of the Shared Associative Memory (SAM) framework introduced in the following section.

## 4. Distributed HTM Framework (D-HTM)

### 4.1. Cross-Entity Representation Alignment

A fundamental challenge in cross-entity anomaly warning is that similar physical events may appear substantially different across monitored entities. For example, a sudden increase in CPU utilization may represent a severe deviation on a machine that normally operates at 20% load, while the same increase may be routine for another machine operating at 70% load. Direct comparison of raw measurements therefore suffers from operating-point bias and can obscure shared precursor patterns.

To reduce this bias, each feature is independently normalized using z-score normalization. For entity  $i$  and feature  $j$ , the normalized value is

$$z_{i,j}(t) = \frac{x_{i,j}(t) - \mu_{i,j}}{\sigma_{i,j}}, \quad (1)$$

where  $\mu_{i,j}$  and  $\sigma_{i,j}$  are computed from the training portion of the corresponding entity’s data and remain fixed throughout evaluation. The result-

ing normalized features describe deviations relative to each entity’s normal operating regime rather than absolute measurement values, making similar behaviors more directly comparable.

Normalization alone, however, is insufficient. If each entity trains an independent Spatial Pooler (SP), similar normalized inputs may still activate different SDR columns because the learned column assignments evolve independently. Consequently, overlap between SDRs from different entities would no longer reflect semantic similarity.

To overcome this limitation, all entities share a single Spatial Pooler. The shared SP is trained once using representative historical data and then frozen, ensuring that comparable input patterns generate overlapping sparse representations regardless of their source entity. Together, z-score normalization and the shared SP establish a common SDR space that enables reliable overlap-based comparison and forms the foundation of the Shared Associative Memory.

#### 4.2. System Architecture

Having established a common representation space, we now describe the overall Distributed HTM (D-HTM) framework. D-HTM consists of  $N$  distributed HTM agents that share a Spatial Pooler and a Shared Associative Memory (SAM), while maintaining independent Temporal Memory (TM) modules for local sequence learning. An overview of the architecture is shown in Fig. 3.

For each entity  $i$ , an incoming multivariate data stream  $X_i(t)$  is normalized, encoded into Sparse Distributed Representations (SDRs), and processed by the shared Spatial Pooler. The resulting sparse representation is supplied to the local Temporal Memory, which learns entity-specific temporal dynamics and computes anomaly scores from prediction errors.

When a local anomaly onset is detected, the preceding  $L$  Spatial Pooler activations are extracted and stored in SAM as a precursor memory,

$$M_j = \{s_{t-L}, s_{t-L+1}, \dots, s_{t-1}\}, \quad (2)$$

where each  $s_t$  denotes the active Spatial Pooler columns at time  $t$ . The lookback horizon  $L$  determines the amount of temporal context stored before anomaly onset and is treated as a dataset-dependent parameter. Its influence on warning performance is evaluated in Section 5.3.3.

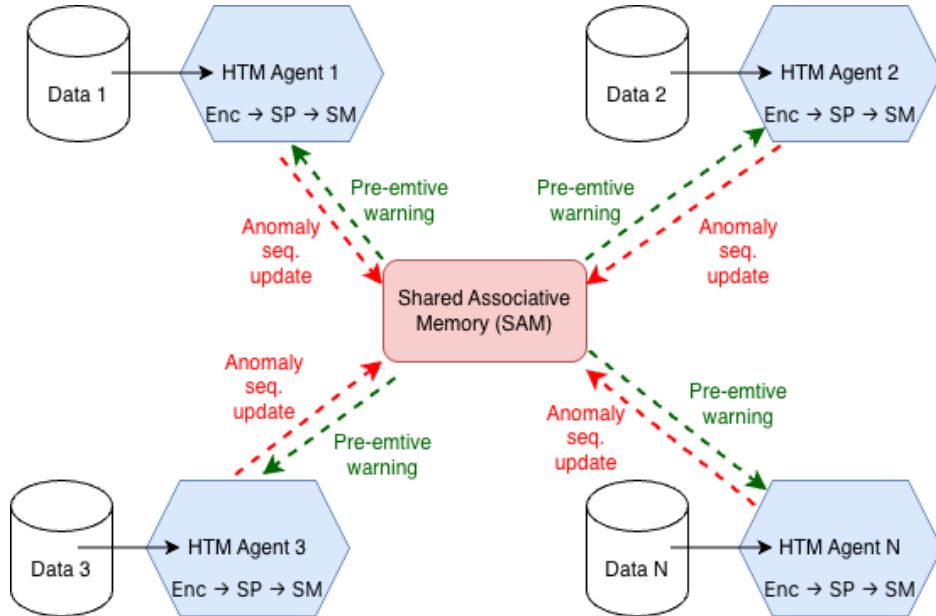


Figure 3: Overview of the Distributed HTM (D-HTM) framework. Each entity processes a local data stream through z-score normalization, an encoder, a shared Spatial Pooler (SP), and a local Temporal Memory (TM). Precursor memories extracted before anomaly onset are stored in the Shared Associative Memory (SAM), enabling cross-entity warning propagation through memory retrieval.

Overall, D-HTM combines localized temporal learning with a shared repository of precursor memories. Each agent continues to learn independently from its own data stream while contributing to and querying SAM during online operation. The memory formation, retrieval, and update procedures are described in Section 4.4.

#### 4.3. Shared Spatial Pooler

To enable cross-entity comparison, D-HTM replaces the conventional per-entity Spatial Pooler (SP) with a single Shared Spatial Pooler.

The Shared SP is trained once using the combined normal operating data from all monitored entities during an offline initialization stage. After convergence, its parameters are frozen and reused by every HTM agent throughout deployment, while each agent maintains an independent Temporal Memory for online sequence learning.

Because all agents share the same Spatial Pooler, similar normalized inputs are projected into comparable Sparse Distributed Representations

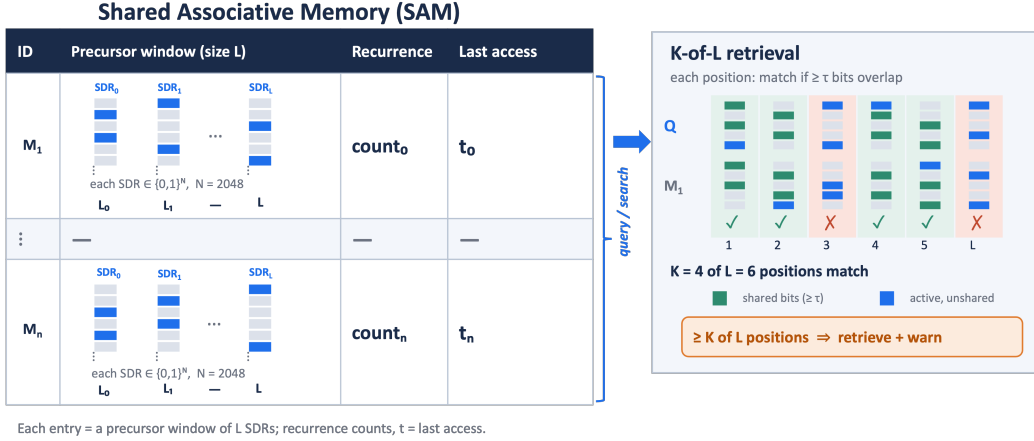


Figure 4: Structure of the Shared Associative Memory (SAM) and its retrieval process. Each memory entry stores a precursor window of  $L$  Spatial Pooler SDRs together with its recurrence count ( $n$ ) and last-access time ( $t$ ). During inference, the current query window is compared against stored memories using K-of- $L$  sparse overlap matching. A warning is issued when at least  $K$  of the  $L$  corresponding SDRs satisfy the overlap threshold  $\tau$ .

(SDRs) regardless of their source entity. Consequently, precursor patterns generated by different entities can be compared directly using sparse overlap without requiring alignment of raw feature values or entity-specific SP representations.

Only the feature representation is shared. Temporal learning remains localized within each Temporal Memory, allowing every entity to adapt to its own sequential dynamics while benefiting from a common sparse representation for cross-entity precursor retrieval.

#### 4.4. Shared Associative Memory and Warning Propagation

Once a common representation has been established by the Shared Spatial Pooler, recurring precursor patterns can be stored in a shared memory and reused across entities. This functionality is provided by the Shared Associative Memory (SAM), illustrated in Fig. 4, which stores activation patterns that have previously preceded anomaly onset.

Each memory entry consists of a precursor activation window together with metadata describing its usage history,

$$M_j = (W_j, n_j, t_j), \quad (3)$$

where  $W_j = \{w_j^0, w_j^1, \dots, w_j^{L-1}\}$  denotes the stored precursor window,  $n_j$  records the recurrence count, and  $t_j$  stores the most recent access time. The recurrence count serves as a confidence measure, reflecting how frequently the same precursor has been observed across all monitored entities.

Whenever a local anomaly onset is detected, the preceding  $L$  Spatial Pooler activation patterns are extracted and compared with existing entries in SAM. If a sufficiently similar memory already exists, its recurrence count is incremented; otherwise, a new memory entry is created. This reinforcement mechanism prevents duplicate memories while naturally increasing the confidence of frequently recurring precursor patterns.

During inference, each entity continuously constructs a query window from its most recent Spatial Pooler activations,

$$Q_t = \{q_{t-L}, q_{t-L+1}, \dots, q_{t-1}\}. \quad (4)$$

For every stored memory, corresponding SDRs are compared position by position. A positional match is declared whenever

$$|q^p \cap w_j^p| \geq \tau, \quad (5)$$

where  $q^p$  denotes the query SDR,  $w_j^p$  denotes the stored SDR at the same position, and  $\tau$  specifies the minimum overlap required for two SDRs to be considered similar. In this work,  $\tau$  remains fixed across all experiments.

A precursor memory is retrieved when at least  $K$  of the  $L$  positions satisfy Eq. (5),

$$\text{warning}(t) = \max_j \left( \sum_{p=0}^{L-1} \mathbf{1} [ |q^p \cap w_j^p| \geq \tau ] \right) \geq K, \quad (6)$$

where  $K$  controls the minimum number of matching positions required to issue a warning. Larger values of  $K$  demand stronger temporal agreement, while smaller values permit more tolerant retrieval.

Retrieved memories contribute evidence toward a pre-emptive warning before the local anomaly detector signals an anomaly. The recurrence count reflects the historical reliability of each precursor, while the last-access timestamp supports memory management. When the memory reaches its capacity, entries with low recurrence counts and long periods of inactivity are preferentially removed, allowing frequently reused precursor memories to remain while obsolete patterns are gradually forgotten.

---

**Algorithm 1:** Shared Associative Memory (SAM) Retrieval and Update

---

**Input:** Current SDR  $s(t)$ , lookback horizon  $L$ , overlap threshold  $\tau$ , match threshold  $K$ , shared memory  $\mathcal{M}$

**Output:** Pre-emptive warning

Form query window  $Q_t = \{s(t-L), \dots, s(t-1)\}$ ;

**foreach** memory  $M_j = (W_j, n_j, t_j) \in \mathcal{M}$  **do**

- Compute the number of matching positions between  $Q_t$  and  $W_j$ ;
- if** at least  $K$  positions satisfy  $|q^p \cap w_j^p| \geq \tau$  **then**
  - Issue warning;
  - Update last-access timestamp  $t_j \leftarrow t$ ;

**if** local HTM detects anomaly onset **then**

- Extract precursor window  $W = \{s(t-L), \dots, s(t-1)\}$ ;
- if**  $W$  matches an existing memory **then**
  - Increment recurrence count  $n_j \leftarrow n_j + 1$ ;
  - Update last-access timestamp  $t_j \leftarrow t$ ;
- else**
  - Insert new memory  $(W, 1, t)$  into  $\mathcal{M}$ ;

**if** memory capacity exceeded **then**

- Remove memories with the lowest recurrence count and oldest last-access time;

---

Algorithm 1 summarizes the complete online operation of SAM. At every timestep, memory retrieval is performed before any new memory is inserted, ensuring that warnings are generated exclusively from precursor patterns learned during previous anomaly events.

Because  $L$  is measured in samples rather than physical time, the effective precursor horizon depends on the sampling interval and failure development characteristics of each dataset. Consequently, the optimal value of  $L$  is dataset dependent and is investigated in Section 5.3.3.

## 5. Experiments and Discussion

### 5.1. Datasets and Preprocessing

We evaluate the proposed framework on three established multi-variate anomaly detection benchmarks—SMD [15], SMAP [40], and MSL [40]—together with a synthetic cascade dataset designed to evaluate controlled cross-entity warning propagation. SMD contains monitoring traces from multiple production servers, while SMAP and MSL comprise NASA spacecraft telemetry collected from multiple related channels. The synthetic dataset provides a controlled environment in which precursor trajectories are intentionally shared across entities, enabling evaluation of the upper bound of transferable warning performance. Dataset statistics are summarized in Table 2.

Table 2: Dataset summary. Steps are reported per entity; anomaly statistics are computed over the test split only.

Dataset	Entities	Features	Train Steps	Test Steps	Anomaly Events
SMD [15]	28	38	~28,000	~28,000	327
SMAP [40]	54 <sup>a</sup>	25	312–2,881	4,453–8,640	68
MSL [40]	27	55	439–4,308	1,096–6,100	36
Synthetic (ours)	6	15	5,000	5,000	24

Preprocessing is performed independently for each entity to prevent information leakage. All feature statistics are computed exclusively from the training split and remain fixed throughout evaluation. Each feature is z-score normalized using its training-set mean and standard deviation. Normalization is applied per machine for SMD, per telemetry channel for SMAP and MSL, and per node for the synthetic dataset. Features with near-zero variance ( $\sigma < 10^{-8}$ ) are mapped to zero, and normalized values are clipped to  $[-10, 10]$  prior to encoding.

For SMD, we follow the standard train/test protocol of Omni-Anomaly [15]. The first half of each machine trace is used for training and the second half for testing. For SMAP and MSL, we use the official Telemanom [40] train/test splits. Three SMD machines (machine-2-4, machine-3-1, and machine-3-3) are excluded because their normalized pre-anomaly profiles become numerically degenerate, producing unstable similarity estimates.

## 5.2. Implementation Details

Unless otherwise stated, identical encoder, Spatial Pooler (SP), and Temporal Memory (TM) configurations are used across all real-world datasets to preserve consistent Sparse Distributed Representation (SDR) statistics during cross-entity retrieval. The complete implementation parameters are summarized in Table 3.

Each scalar feature is encoded using a 512-bit `ScalarEncoder` with 41 active bits. Per-feature encodings are concatenated before Spatial Pooling, yielding an expected random SDR overlap of approximately 1.64 bits, which serves as the effective noise floor for overlap-based retrieval.

The shared SP contains 1,024 mini-columns with a target sparsity of 4% ( $\approx 41$  active columns) and uses global inhibition. It is trained offline for one epoch using shuffled training data and then frozen during inference, preserving consistent SDR semantics across all entities. Each entity maintains an independent TM that continues online learning throughout inference. Prediction errors are converted into anomaly scores and smoothed using a rolling mean prior to thresholding.

Four TM hyperparameters are optimized independently for each dataset using Optuna [41] with 40 optimization trials, maximizing the mean point-adjust F1 on the validation set. The search includes `boostStrength`, `cellsPerColumn`, `activationThreshold`, and `predictedSegmentDecrement`. Hyperparameter optimization is performed on the USF CIRCE HPC cluster.

For all datasets, the final 20% of the training split is reserved for validation. Hyperparameter optimization and lookback-horizon selection are performed exclusively on this validation subset. After parameter selection, the model is retrained using the complete training data and evaluated once on the held-out test set. Test labels are never used during parameter tuning or lookback selection.

Memory insertion follows a strictly online protocol. At each timestep, SAM first queries the shared memory using only information available up to the current time. If the local HTM detector subsequently identifies an anomaly onset, the preceding  $L$  Spatial Pooler activations are stored as a precursor memory. Ground-truth anomaly labels are used exclusively for evaluation and are never available during memory formation or retrieval, ensuring a leakage-free online evaluation.

We compare D-HTM against three baselines. `OmniAnomaly` [15] serves as the primary deep-learning baseline following the standard SMD/SMAP/MSL

evaluation protocol. A single-entity HTM baseline isolates the contribution of the shared SP by running HTM independently for each entity without cross-entity communication. Finally, an encoder-only D-HTM ablation replaces SP outputs with raw `ScalarEncoder` bit arrays to evaluate the importance of learned sparse representations for transferable precursor matching.

Performance is evaluated using Precision, Recall, and F1 under the point-adjust protocol [15]. For cross-entity warning evaluation, we additionally report Warning Precision, Event Recall, Mean Lead Time, and warning confidence.

The benchmark datasets contain relatively few anomaly events, resulting in far fewer precursor memories than the configured SAM capacity. Consequently, memory eviction is rarely triggered during the reported experiments. The recurrence- and recency-based replacement policy is primarily intended for long-running deployments where memory growth eventually exceeds the available capacity.

### 5.3. Experimental Results

#### 5.3.1. Reactive Anomaly Detection Performance

Before evaluating cross-entity warning generation, we first assess the reactive anomaly detection performance of the underlying HTM detector. Since D-HTM extends conventional HTM through shared associative memory, it is important to establish that the underlying Temporal Memory provides a competitive foundation for anomaly detection.

Table 4 compares point-adjust Precision, Recall, and F1 between Omni-Anomaly and independently trained single-entity HTM models on the SMD, SMAP, and MSL benchmarks. Each HTM model is trained and evaluated independently for each entity without any cross-entity communication.

HTM achieves competitive reactive anomaly detection performance across all three benchmarks, validating its suitability as the temporal reasoning component of D-HTM. Although the primary objective of this work is cross-entity warning generation, local HTM detections determine when new precursor memories are inserted into SAM. Consequently, the quality of the underlying detector directly influences the quality of the learned precursor memory.

Having established the effectiveness of the underlying HTM detector, we next evaluate whether the proposed shared representation enables transferable precursor retrieval and cross-entity warning generation.

Table 3: Implementation parameters used across experiments.

Parameter	Value
Encoder size	512 bits
Encoder active bits	41
Encoder input range	[-10,10] (z-score)
Expected random SDR overlap	1.64 bits
SP columns	1,024
SP sparsity	4%
SP inhibition	Global
SP training	1 offline epoch
SP inference	Frozen
potentialPct	0.85
synPermInactiveDec	0.006
synPermActiveInc	0.04
synPermConnected	0.14
TM inference	Online learning enabled
initialPermanence	0.21
minThreshold	10
maxNewSynapseCount	32
permanenceIncrement	0.10
permanenceDecrement	0.10
maxSegmentsPerCell	128
maxSynapsesPerSegment	64
Optuna trials	40
Optimization objective	Mean point-adjust F1
Lookback horizon ( $L$ )	Dataset dependent
Match ratio search ( $K/L$ )	{0.20, 0.40, 0.60, 0.80, 1.00}
Anomaly score smoothing	150 steps

Table 4: Reactive anomaly detection performance of the underlying single-entity HTM detector compared with OmniAnomaly. HTM detections are used to trigger memory insertion into SAM during online operation.

Dataset	Method	Precision	Recall	F1
SMD	OmniAnomaly [15]	0.838	0.923	0.879
	Single-entity HTM	0.789	0.842	0.815
SMAP	OmniAnomaly [15]	0.882	0.940	0.910
	Single-entity HTM	0.812	0.873	0.841
MSL	OmniAnomaly [15]	0.858	0.926	0.891
	Single-entity HTM	0.756	0.884	0.815

Table 5: Representation ablation study averaged across the three real-world datasets. Results are macro-averaged over SMD, SMAP, and MSL using the same warning evaluation protocol as Table 6.

Representation	Precision	Recall	F1
Raw Features	0.18	0.79	0.29
Encoder SDR	0.34	0.84	0.48
Per-Entity SP	0.58	0.86	0.69
Shared SP	0.73	0.98	0.82

### 5.3.2. Shared Representation and Cross-Entity Warning Performance

We first evaluate the importance of representation alignment through a representation-level ablation study. Warning retrieval is performed using four alternative representations: (i) raw normalized features, (ii) encoder SDRs, (iii) independently trained per-entity Spatial Poolers (SPs), and (iv) the proposed shared SP.

Table 5 reports macro-averaged warning performance across SMD, SMAP, and MSL. The synthetic benchmark is excluded because its intentionally shared precursor structure would artificially inflate representation transferability.

The results demonstrate that representation alignment is essential for cross-entity warning retrieval. Raw features and encoder SDRs preserve local information but lack a sufficiently structured representation for reliable matching, while independently trained SPs produce entity-specific SDRs that limit transferability. In contrast, the shared SP consistently achieves the highest performance by mapping similar behaviors to overlapping sparse representations.

Having established the importance of the shared representation, we next evaluate warning generation across both real-world and synthetic datasets.

Table 6 summarizes cross-entity warning performance. Across all datasets, SAM consistently generates warnings before local anomaly onset by retrieving previously observed precursor memories.

SMD represents the most challenging environment, achieving high recall but lower precision due to greater inter-machine heterogeneity and less consistent precursor structure. In contrast, SMAP and MSL exhibit more transferable precursor dynamics, resulting in substantially higher precision. The synthetic cascade achieves the strongest overall performance because its

Table 6: Cross-entity warning performance across real-world and synthetic datasets.  $N$  denotes the number of monitored entities,  $L$  is the lookback horizon,  $K$  is the minimum number of matching positions required for retrieval, and Warnings/Entity is the average number of warnings generated per monitored entity.

Dataset	$N$	$L$	$K$	Warnings per			Avg. Lead	
				Entity	Prec.	Rec.	F1	Time
SMD	28	5	3	31	0.48	0.91	0.63	3.42
SMAP	54	10	6	11	0.81	0.91	0.86	6.87
MSL	27	10	6	7	0.85	0.94	0.89	7.21
Synthetic	6	15	9	4	0.90	0.96	0.93	11.36

precursor trajectories are intentionally shared across entities.

The selected lookback horizons also reflect differences in precursor development. SMD performs best with a short precursor horizon ( $L = 5$ ), whereas SMAP and MSL benefit from a longer context ( $L = 10$ ). The synthetic cascade achieves its highest performance with  $L = 15$ , consistent with its designed multi-step precursor evolution.

Figure 5 illustrates representative warning trajectories for SMD, SMAP, and MSL. In each case, SAM retrieves precursor memories several samples before local anomaly onset. Similar behavior is observed in the synthetic benchmark, demonstrating that shared sparse representations and associative memory enable transferable cross-entity early warning generation.

Across all evaluated datasets, SAM consistently retrieves precursor memories before local anomaly onset, providing actionable lead time for preventive intervention. The representative trajectories illustrate how shared sparse representations enable transferable cross-entity warning generation.

### 5.3.3. Robustness and Validation Studies

To evaluate the robustness of SAM, we investigate its sensitivity to the lookback horizon and retrieval strictness. We also perform a shuffled-control experiment to verify that warning generation depends on meaningful precursor structure rather than accidental SDR overlap.

**(a) Lookback Horizon Sensitivity:** The lookback horizon  $L$  determines how many Spatial Pooler activation patterns are stored before anomaly onset. A short horizon may fail to capture sufficient precursor context, whereas an excessively long horizon can introduce unnecessary matching constraints and reduce retrieval specificity. Because  $L$  is measured in samples and each dataset exhibits different temporal characteristics, the optimal precursor

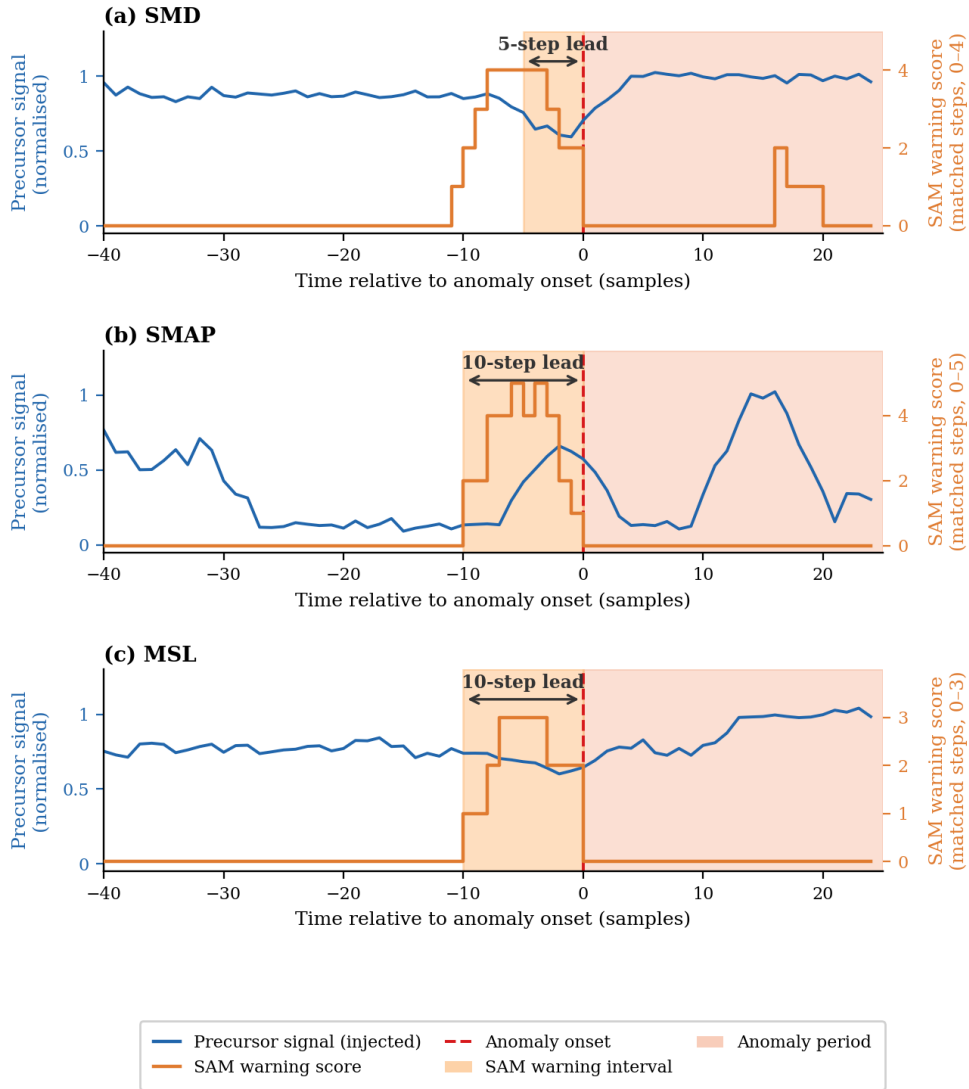


Figure 5: Representative warning trajectories for SMD, SMAP, and MSL. Each panel overlays the precursor signal and the SAM warning score relative to anomaly onset. Warnings are generated several timesteps before anomaly onset, illustrating retrieval of transferable precursor memories.

horizon is dataset dependent.

Table 7 shows that SMD achieves its best performance with short precursor windows, indicating that transferable precursor information occurs close

Table 7: Lookback horizon sensitivity across datasets. For each value of  $L$ , the retrieval threshold is fixed at  $K = \lceil 0.6L \rceil$ . Increasing  $L$  improves warning performance until the dominant precursor horizon of each system is captured, after which additional context may reduce retrieval specificity.

Dataset	$L$	$K$	Precision	Recall	F1	Lead Time
SMD	5	3	0.48	0.91	0.63	3.42
SMD	10	6	0.44	0.89	0.59	5.86
SMD	15	9	0.41	0.86	0.56	7.24
SMD	20	12	0.39	0.82	0.53	8.10
SMAP	5	3	0.76	0.88	0.82	3.94
SMAP	10	6	0.81	0.91	0.86	6.87
SMAP	15	9	0.79	0.90	0.84	8.36
SMAP	20	12	0.77	0.87	0.82	9.45
MSL	5	3	0.79	0.90	0.84	4.12
MSL	10	6	0.85	0.94	0.89	7.21
MSL	15	9	0.84	0.92	0.88	8.74
MSL	20	12	0.81	0.90	0.85	9.62
Synthetic	5	3	0.84	0.89	0.86	4.21
Synthetic	10	6	0.88	0.93	0.90	8.74
Synthetic	15	9	0.90	0.96	0.93	11.36
Synthetic	20	12	0.89	0.95	0.92	12.08

to anomaly onset. In contrast, SMAP and MSL benefit from longer horizons, while the synthetic benchmark achieves its highest performance with  $L = 15$ , consistent with its designed multi-step precursor evolution. Based on these validation results, the selected operating horizons are  $L = 5$  for SMD,  $L = 10$  for SMAP and MSL, and  $L = 15$  for the synthetic benchmark. Warning performance is evaluated at the event level rather than the point level. A single anomaly detected by the local HTM detector inserts one precursor memory into SAM, but that memory may subsequently generate warnings for multiple future anomaly events across different entities. Consequently, warning recall is not expected to be bounded by the point-wise recall of the underlying detector.

**(b) K-of-L Retrieval Sensitivity:** We next evaluate the effect of retrieval strictness. Smaller values of  $K$  increase recall at the expense of precision, whereas larger values require stronger temporal agreement and therefore improve precision while reducing recall. Because the selected lookback horizon

Table 8: K-of- $L$  retrieval sensitivity across datasets. For each dataset,  $L$  is fixed to the selected lookback horizon used in Table 6, while  $K$  is varied as a fraction of  $L$ . The selected operating point is shown in bold.

Dataset	$L$	Match Ratio ( $K/L$ )	$K$	Precision	Recall	F1
SMD	5	0.20	1	0.34	0.99	0.51
SMD	5	0.40	2	0.41	0.98	0.58
SMD	5	<b>0.60</b>	<b>3</b>	<b>0.46</b>	<b>0.97</b>	<b>0.62</b>
SMD	5	0.80	4	0.51	0.79	0.61
SMD	5	1.00	5	0.58	0.54	0.56
SMAP	10	0.20	2	0.63	0.99	0.77
SMAP	10	0.40	4	0.76	0.97	0.85
SMAP	10	<b>0.60</b>	<b>6</b>	<b>0.84</b>	<b>0.96</b>	<b>0.90</b>
SMAP	10	0.80	8	0.89	0.78	0.83
SMAP	10	1.00	10	0.94	0.49	0.64
MSL	10	0.20	2	0.66	1.00	0.80
MSL	10	0.40	4	0.80	1.00	0.89
MSL	10	<b>0.60</b>	<b>6</b>	<b>0.89</b>	<b>0.99</b>	<b>0.94</b>
MSL	10	0.80	8	0.92	0.81	0.86
MSL	10	1.00	10	0.96	0.52	0.67
Synthetic	15	0.20	3	0.71	1.00	0.83
Synthetic	15	0.40	6	0.84	0.99	0.91
Synthetic	15	<b>0.60</b>	<b>9</b>	<b>0.92</b>	<b>0.98</b>	<b>0.95</b>
Synthetic	15	0.80	12	0.95	0.82	0.88
Synthetic	15	1.00	15	0.98	0.57	0.72

differs across datasets, retrieval strictness is expressed as the match ratio  $K/L$ .

Table 8 exhibits the expected precision–recall trade-off. Highly permissive retrieval generates more false warnings, whereas exact matching misses transferable precursor variants. A match ratio of  $K/L = 0.60$  consistently provides the best balance and is therefore used in all subsequent experiments. **(c) Shuffled Control Experiment:** Finally, we perform a shuffled-control experiment by randomly reassigning stored precursor memories before retrieval while leaving all other components unchanged.

The shuffled-control experiment reduces the macro-averaged warning F1

Table 9: Shuffled-control validation. Results are macro-averaged across SMD, SMAP, and MSL. Random reassignment of stored precursor signatures causes warning performance to collapse, indicating that retrieval depends on meaningful precursor structure rather than accidental SDR overlap.

Method	Precision	Recall	F1
Normal SAM	0.73	0.98	0.82
Shuffled SAM	0.05	0.06	0.05

from 0.82 to 0.05, confirming that successful retrieval depends on meaningful precursor memories preserved by the shared SDR representation rather than accidental overlap. Together, these studies demonstrate that SAM is robust across a broad range of parameter settings and derives its warning capability from transferable precursor structure.

## 6. Discussion & Conclusion

This paper introduced Distributed Hierarchical Temporal Memory (D-HTM), a distributed anomaly detection framework that augments conventional HTM agents with a shared Spatial Pooler (SP) and a Shared Associative Memory (SAM). By combining a common sparse representation with a shared memory of recurring precursor patterns, the proposed framework enables knowledge learned by one entity to contribute to early warning generation on related entities without requiring centralized sequence models or parameter sharing.

Experimental results demonstrate that D-HTM extends the strong reactive anomaly detection capability of HTM with effective cross-entity warning generation. Representation ablation studies show that a shared Spatial Pooler is essential for transferable precursor retrieval, while the shuffled-control experiment confirms that warning generation depends on meaningful precursor structure rather than accidental SDR overlap. Across both real-world and synthetic datasets, SAM consistently generated warnings before local anomaly onset, demonstrating the feasibility of distributed precursor sharing.

The current framework has several limitations. SAM employs a fixed lookback horizon and overlap-based retrieval without explicit causal reasoning or probabilistic confidence estimation. In addition, the Spatial Pooler remains frozen after offline training to preserve stable SDR semantics, prevent-

ing representation adaptation during deployment. Future work will investigate adaptive lookback windows, online representation learning, graph-aware communication, and confidence-aware retrieval strategies for large-scale distributed monitoring systems.

Overall, this work demonstrates that transferable precursor memories can enable cooperative early warning while preserving HTM’s online learning capability. We believe these results provide a promising foundation for future research in distributed anomaly detection and cooperative multi-agent temporal reasoning.

### **Declaration of generative AI and AI-assisted technologies in the manuscript preparation process**

During the preparation of this work, the author used ChatGPT and Claude LLM models to improve language clarity and readability. After using this tool, the author reviewed and edited the content as needed and takes full responsibility for the content of the publication.

### **Data Availability Statement**

The datasets generated or analyzed during the current study are available from the corresponding author on reasonable request.

### **References**

- [1] J. E. Laird, C. Lebiere, P. S. Rosenbloom, A standard model of the mind: Toward a common computational framework across artificial intelligence, cognitive science, neuroscience, and robotics, *AI Magazine* 38 (4) (2017) 13–26.
- [2] J. Hawkins, S. Ahmad, Why neurons have thousands of synapses, a theory of sequence memory in neocortex, *Frontiers in Neural Circuits* 10 (2016) 23. doi:10.3389/fncir.2016.00023.
- [3] S. Ahmad, J. Hawkins, How do neurons operate on sparse distributed representations? a mathematical theory of sparsity, neurons and active dendrites, arXiv preprint arXiv:1601.00720 (2016).

- [4] A. Lavin, S. Ahmad, Evaluating real-time anomaly detection algorithms—the numenta anomaly benchmark, in: IEEE 14th International Conference on Machine Learning and Applications (ICMLA), 2015, pp. 38–44. doi:10.1109/ICMLA.2015.141.
- [5] F. Zhou, H. Yang, Y. Zhai, S. Chen, Hierarchical temporal memory for medical image classification, IEEE Access 6 (2018) 30750–30758. doi:10.1109/ACCESS.2018.2844115.
- [6] T. Adam, M. Haase, H. Bernhard, Wafer defect classification using hierarchical temporal memory, Microelectronics Reliability 88–90 (2018) 1027–1031. doi:10.1016/j.microrel.2018.06.053.
- [7] S. James, S. Bhanja, Htm-based biometric recognition system for real-time identity verification, Pattern Recognition Letters 92 (2017) 102–108. doi:10.1016/j.patrec.2017.05.018.
- [8] P. Neubert, P. Protzel, Sequence-based place recognition using hierarchical temporal memory, IEEE Transactions on Neural Networks and Learning Systems 29 (9) (2018) 4122–4132. doi:10.1109/TNNLS.2017.2773578.
- [9] M. Micheletto, L. Garrido, G. Ruiz, Using htm for earthquake prediction from seismic sensor data, IEEE Transactions on Geoscience and Remote Sensing 56 (12) (2018) 7342–7350. doi:10.1109/TGRS.2018.2844083.
- [10] E. Osegi, A. Usman, M. Ogbimi, Using hierarchical temporal memory for short-term power load forecasting, Neural Computing and Applications 30 (11) (2018) 3451–3463. doi:10.1007/s00521-017-2928-4.
- [11] A. Ziyarah, D. Kudithipudi, End-to-end neuromemristive architecture for hierarchical temporal memory, IEEE Transactions on Neural Networks and Learning Systems 31 (8) (2020) 2703–2715. doi:10.1109/TNNLS.2019.2932783.
- [12] I. Bautista, S. Sarkar, S. Bhanja, Matlabhtm: A sequence memory model of neocortical layers for anomaly detection, SoftwareX 11 (2020) 100491. doi:10.1016/j.softx.2020.100491.

- [13] K. D. Harris, G. M. G. Shepherd, The neocortical circuit: themes and variations, *Nature Neuroscience* 18 (2) (2015) 170–181. doi:10.1038/nn.3917.
- [14] J. Audibert, P. Michiardi, F. Guyard, S. Marti, M. A. Zuluaga, USAD: Unsupervised anomaly detection on multivariate time series, in: *Proceedings of the 26th ACM SIGKDD International Conference on Knowledge Discovery & Data Mining*, ACM, 2020, pp. 3395–3404.
- [15] Y. Su, Y. Zhao, C. Niu, R. Liu, W. Sun, D. Pei, Robust anomaly detection for multivariate time series through stochastic recurrent neural network, in: *Proceedings of the 25th ACM SIGKDD International Conference on Knowledge Discovery & Data Mining*, 2019, pp. 2828–2837. doi:10.1145/3292500.3330672.
- [16] J. N. Foerster, Y. M. Assael, N. de Freitas, S. Whiteson, Learning to communicate with deep multi-agent reinforcement learning, in: *Advances in Neural Information Processing Systems*, Vol. 29, 2016, pp. 2137–2145.  
URL <https://arxiv.org/abs/1605.06676>
- [17] A. A. Rusu, N. C. Rabinowitz, G. Desjardins, H. Soyer, J. Kirkpatrick, K. Kavukcuoglu, R. Pascanu, R. Hadsell, Progressive neural networks, *arXiv preprint arXiv:1606.04671* (2016).  
URL <https://arxiv.org/abs/1606.04671>
- [18] R. Vashist, C. Mueller, Distributed memory architectures in multi-agent systems, *tech Report* (2020).
- [19] M. Shoybi, M. Patwary, R. Puri, et al., Megatron-lm: Training multi-billion parameter language models using model parallelism, in: *arXiv preprint arXiv:1909.08053*, 2019.
- [20] A. Tampuu, T. Matiisen, I. Kuzovkin, et al., Multi-agent cooperation and competition with deep reinforcement learning, in: *arXiv preprint arXiv:1511.08779*, 2015.
- [21] H. B. McMahan, E. Moore, D. Ramage, S. Hampson, B. A. y Arcas, Communication-efficient learning of deep networks from decentralized data, in: *Proceedings of the 20th International Conference on Artificial*

Intelligence and Statistics (AISTATS), Vol. 54, PMLR, 2017, pp. 1273–1282.

- [22] J. Hao, P. Chen, J. Chen, X. Li, Multi-task federated learning-based system anomaly detection and multi-classification for microservices architecture, *Future Generation Computer Systems* 159 (2024) 77–90. doi:10.1016/j.future.2024.05.001.
- [23] J. Hao, P. Chen, J. Chen, X. Li, Effectively detecting and diagnosing distributed multivariate time series anomalies via unsupervised federated hypernetwork, *Information Processing & Management* (2025). doi:10.1016/j.ipm.2025.103974.
- [24] L. Zheng, et al., MAS-LSTM: A multi-agent LSTM-based approach for scalable anomaly detection in IIoT networks, *Processes* 13 (3) (2025) 753. doi:10.3390/pr13030753.
- [25] T. Yang, J. Liu, W. Siu, J. Wang, Z. Qian, et al., AD-AGENT: A multi-agent framework for end-to-end anomaly detection, *arXiv preprint arXiv:2505.12594* (2025).
- [26] Anonymous, LEMAD: LLM-empowered multi-agent system for anomaly detection in power grid services, *Electronics* 14 (15) (2025) 3008. doi:10.3390/electronics14153008.
- [27] J. Hawkins, S. Ahmad, Hierarchical temporal memory including htm cortical learning algorithms, *Tech. rep.*, Numenta (2016). URL <https://numenta.org/resources/white-papers/>
- [28] S. Ahmad, J. Hawkins, How do neurons operate on sparse distributed representations? A mathematical theory of sparsity, neurons and active dendrites, *arXiv preprint arXiv:1601.00720* (2016). URL <https://arxiv.org/abs/1601.00720>
- [29] P. Bera, S. H. Moon, J. Adorno, D. A. Reis, S. Bhanja, Enhancing biologically inspired hierarchical temporal memory with hardware-accelerated reflex memory, *arXiv preprint Preprint submitted to Elsevier* (2025).
- [30] J. Shen, W. Ni, Q. Xu, G. Pan, H. Tang, Context gating in spiking neural networks: Achieving lifelong learning through integration of local and global plasticity, *Knowledge-Based Systems* 311 (2025) 112999.

- [31] M. Gatti, J. A. Barbato, C. Zandron, Spiking neural network classification of x-ray chest images, *Knowledge-Based Systems* 314 (2025) 113194.
- [32] M. Davies, N. Srinivasa, T.-H. Lin, G. Chinya, Y. Cao, S. H. Choday, G. Dimou, P. Joshi, N. Imam, S. Jain, Y. Liao, C.-K. Lin, A. Lines, R. Liu, D. Mathaikutty, S. McCoy, A. Paul, J. Tse, G. Venkataramanan, Y.-H. Weng, A. Wild, Y. Yang, H. Wang, Loihi: A neuromorphic many-core processor with on-chip learning, *IEEE Micro* 38 (1) (2018) 82–99. doi:10.1109/MM.2018.112130359.
- [33] M. Thottan, C. Ji, Proactive anomaly detection using distributed intelligent agents, *IEEE Network* 12 (5) (1998) 21–27.
- [34] M.-C. Lee, J.-C. Lin, E. G. Gran, RePAD: Real-time proactive anomaly detection for time series, in: *Proceedings of the 34th International Conference on Advanced Information Networking and Applications (AINA 2020)*, Springer, 2020, pp. 1291–1302. doi:10.1007/978-3-030-44041-1\\_110.
- [35] J. Jeon, J. Park, S. Park, J. Choi, M. Kim, N. Park, Possibility for proactive anomaly detection, *arXiv preprint arXiv:2504.11623* (2025).
- [36] P. Cao, K.-W. Chung, Z. Kalbarczyk, R. Iyer, A. J. Slagell, Preemptive intrusion detection, in: *Proceedings of the 2015 Symposium and Bootcamp on the Science of Security (HotSoS)*, ACM, 2015, p. 21. doi:10.1145/2746285.2746306.
- [37] Anonymous, A novel anomaly detection method for multivariate time series based on spatial-temporal graph learning, *Journal of King Saud University – Computer and Information Sciences* (2025). doi:10.1007/s44443-025-00024-3.
- [38] Z. Li, Y. Zhao, J. Han, Y. Su, R. Jia, Z. Li, D. Pei, Multivariate time series anomaly detection and interpretation using hierarchical inter-metric and temporal embedding, in: *Proceedings of the 27th ACM SIGKDD Conference on Knowledge Discovery & Data Mining*, 2021, pp. 3220–3230. doi:10.1145/3447548.3467075.
- [39] Anonymous, StackVAE: Stacked variational autoencoder for multivariate time series anomaly detection, *AI Open* 3 (2022) 101–110.

- [40] K. Hundman, V. Constantinou, C. Laporte, I. Colwell, T. Soderstrom, Detecting spacecraft anomalies using LSTMs and nonparametric dynamic thresholding, in: Proceedings of the 24th ACM SIGKDD International Conference on Knowledge Discovery & Data Mining, 2018, pp. 387–395. doi:10.1145/3219819.3219845.
- [41] T. Akiba, S. Sano, T. Yanase, T. Ohta, M. Koyama, Optuna: A next-generation hyperparameter optimization framework, in: Proceedings of the 25th ACM SIGKDD International Conference on Knowledge Discovery & Data Mining, 2019, pp. 2623–2631.